Wettability of crushed air-dried minerals

S. D. N. LOURENÇO*, S. K. WOCHE†, J. BACHMANN† and Y. SAULICK*

The importance of soil particle wettability has been recognised in mining engineering, soil science and geomorphology but to a lesser extent in geotechnical engineering, perhaps due to the assumption that soils, or in general most common minerals, are always wettable. From the soil science and geomorphology literature, changes in soil wettability are known to influence soil processes such as infiltration, erosion and post-wildfire debris flows. Organic matter has been identified as one of the most important factors controlling the wettability of natural soils. However, its occurrence is very shallow and often shallower than the depth of interest for geotechnical processes. Therefore, it becomes essential to determine the wettability of minerals, in particular because it can be linked to processes that involve crushing or abrasion of soil particles. This paper examines the wettability of 21 common, freshly crushed minerals (sulfides, oxides and silicates) by measuring wettability via contact angles with the sessile drop method and the Wilhelmy plate method, including particle attributes such as aspect ratio and sphericity. The results revealed a wide range of contact angles for the uncoated minerals, with the sulfides showing strong water-repellent behaviour and the silicates remaining very wettable. Higher contact angles are associated with mineral particles that converge to the shape of a sphere and for those that have a larger aspect ratio.

INTRODUCTION

Commonly occurring minerals are expected to be wettable because the surface free energy of unweathered inorganic soil particles is generally higher than that of water, with an apparent contact angle (CA) of 0°. Mineral engineering has shown some exceptions (e.g. sulfide minerals such as galena or pyrite) that are strongly water repellent (e.g. Prestidge & Ralston, 1995) while commonly occurring minerals such as quartz and calcite are wettable, but with CA values that differ from each other and are higher than the commonly assumed 0° (Hajnos *et al.*, 2013). In the long term, environmental factors may lead to a degradation of mineral surfaces, resulting in changes in wettability. Importantly, particle coatings with organic matter remain the most relevant contributor to soil water repellency (Ma'shum *et al.*, 1988; Doerr *et al.*, 2000).

In natural soils, water repellency impacts hydraulic behaviour, from reduced infiltration and surface runoff (Doerr *et al.*, 2000; Jarvis *et al.*, 2008) to preferential flow (Ritsema & Dekker, 1996). In geotechnical applications, soil wettability is important because suction in unsaturated soils depends not only on the degree of saturation but also on the surface tension and the CAs of the water menisci. Regarding the mechanics and hydraulics of water-repellent soils, the internal friction angle is not affected in wax-coated sands (Bardet *et al.*, 2011) but is reduced in synthetic water-repellent soils (Byun *et al.*, 2011). Soil water retention is reduced for soils with low wettability (Lourenço *et al.*, 2015).

Several soil wettability determination methods have been developed and tested in soil science (e.g. Bachmann *et al.*,

2003). They operate on different working principles and measure dynamic or static CAs using different sample preparation methods. The sessile drop method (SDM) and the Wilhelmy plate method (WPM), which measure CAs for the entire range from 0° to >90° for samples from similar preparation methods, are considered here.

Given the fundamental importance of wettability to geotechnical processes that involve clean mineral particles generated by crushing or abrasion, a comprehensive study of mineral wettability is needed. In this work, the wettability of samples of crushed minerals from three major groups (silicates, oxides and sulfides) was measured using both the SDM and WPM. In particular, the wettability of the minerals (with no particulate organic matter) and the effect of the crushed mineral shape were investigated.

MATERIALS AND METHODS

Minerals

A set of commonly occurring minerals and rocks was selected from the mineral collection of Cardiff University, UK (Table 1). The selected minerals were grouped into silicates such as quartz and feldspar (among the most common in soils), oxides such as hematite and cassiterite (a by-product of chemical weathering) and sulfides (mineral ores from specific geological settings) (Table 1). The crushed rocks represent an assemblage of different minerals.

Mineral samples of mass 50–100 g were cleaned, cut into slices of ~1 cm thickness, washed with deionised water to remove dust, allowed to dry at a temperature of 30°C (because the water repellency of natural soils is temperature dependent (Diehl *et al.*, 2014)) and then crushed in a jaw crusher. The resulting material was gravel-sized, and therefore unsuitable for CA measurements. To reduce the size further, sub-samples were crushed in a ball mill (Retsch PM 400; Haan, Germany). Both the jaw crusher and the mill were cleaned with acetone before use. Lastly, the minerals

Lourenço, Woche, Bachmann and Saulick

Table 1. Mineral composition, particle attributes and CAs determined by SDM and WPM for the tested minerals, ranked in descending order of initial SDM CA

Material			Particle attributes						CA: degrees								WDPT: s $n=3$
									SDM						WPM		
Name	Composition	Category	Size: µm	Number of images analysed	Sphericity	SD	Aspect ratio	SD	Initial $n=6$	SD	1 s $n=6$	SD	5 s $n=6$	SD			
Minerals																	
Galena	PbS	Sulfide	<250	33098	0·759[b]	0·06	0·905[b]	0·13	131·6	4	130·6	3·6	131·1	3·1	164·3		Permanent[c]
Malachite	Cu$_2$CO$_3$(OH)$_2$	Carbonate	<250	42004	0·722[b]	0·05	0·893[b]	0·13	125·4	4·6	125·4	3·5	124·7	3·7	150·5		Permanent[c]
Sphalerite	(Zn,Fe)S	Sulfide	<250	42940	0·723[b]	0·06	0·887[b]	0·12	124·3	5·7	116·4	7·7	111·8	6·6	120·1		30
Iron oxide	—	Oxide	125–250	18927	0·703	0·06	0·841	0·13	99·9	5·6	84·7	11·8	77·9	10·1	96·1		0
Pyrite	FeS$_2$	Sulfide	<250	45442	0·697[b]	0·07	0·875[b]	0·13	99·5	3·8	95·3	7·1	87·3	7·4	112·2		Permanent[c]
Tourmaline	XY$_3$Z$_6$(T$_6$O$_{18}$)(BO$_3$)$_3$V$_3$W	Silicate	<250	NM[a]	NM	NM	NM	NM	98·8	3·5	83·1	4·3	76·4	4·8	101·7		NM
Hematite	Fe$_2$O$_3$	Oxide	<250	3754	0·458	0·11	0·750	0·18	84·9	6·3	58·2	14·8	48·8	14·9	73·5		0
Cassiterite	SnO$_2$	Oxide	<250	14044	0·662	0·07	0·824	0·14	58·9	12·2	33	11·2	25·1	9·9	64·1		0
Calcite	CaCO$_3$	Carbonate	<250	27830	0·656	0·08	0·826	0·14	54·7	3	0	0	0	0	31·1		0
Biotite	K(Mg,Fe)$_3$AlSi$_3$O$_{10}$(F,OH)$_2$	Silicate (mica)	<250	22402	0·585	0·11	0·772	0·17	44·2	7·2	24·3	4·7	14·7	5·5	31·5		0
Olivine	(Mg, Fe)$_2$SiO$_4$	Silicate	<250	NM	NM	NM	NM	NM	32·9	8	0	0	0	NM	11·2		0
Amethyst	SiO$_2$	Silicate	<250	16511	0·634	0·08	0·811	0·15	27·6	5·7	0	0	0	0	0		0
Feldspar	KAlSi$_3$O$_8$	Silicate	<250	32109	0·629	0·08	0·813	0·14	17·2	0	0	0	0	0	0		0
Quartz 2	SiO$_2$	Silicate	<250	NM	NM	NM	NM	NM	NM	NM	NM	NM	NM	NM	5·5		0
Quartz 1	SiO$_2$	Silicate	<250	NM	NM	NM	NM	NM	0	0	0	0	0	0	18		0
Rocks																	
Sandstone	—	Sedimentary rock	<250	32087	0·764	0·05	0·892	0·12	78·5	5·5	64·5	6·1	49·8	7·4	92·3		10·5
Bauxite[d]	—	Al ore	<250	NM	NM	NM	NM	NM	42·4	14·4	0	0	0	0	31·8		NM
Breccia	—	Sedimentary rock	<250	39535	0·670	0·06	0·836	0·13	NM	NM	NM	NM	NM	NM	34·3		NM
Granite	—	Igneous rock	<250	99596	0·655	0·07	0·824	0·14	NM	NM	NM	NM	NM	NM	17·9		NM

[a] Not measured
[b] Particle aspect ratio and sphericity measured in 63–165 µm sized particles
[c] Times exceeding 3 h listed as 'permanent'
[d] Bauxite is a chemical weathering by-product of certain rock types

were sieved (mesh size of 250 μm) and sealed in plastic bags to avoid contamination.

Sessile drop method
To determine the CA, samples were fixed with double-sided adhesive tape on a glass slide as a monolayer of air-dried minerals (particle size <250 μm). It should be noted here that the CA in soils is usually referred to as an apparent CA, as it takes into account the material chemistry, roughness and other effects, and has to be distinguished from the intrinsic CA (related only to material chemistry). Each slide was placed on the CCD equipped contact angle microscope stage (OCA15; DataPhysics Instruments GmbH, Filderstadt, Germany) and a water drop (1 μl) of deionised water was placed onto the sample surface while recording the sequence by video (Goebel *et al.*, 2013). Using SCA 20 software (DataPhysics, Filderstadt, Germany), the CA was obtained from the tangent to the point of the three-phase contact. To assess the time dependency of wettability, the CA was measured from the same video sequence after 30 ms, 1 and 5 s of placement of the drop. For each sample, measurements were conducted for six water drops at room temperature (20±1°C). The water drop penetration time (WDPT), an index test, was also determined to assess the time decay of water repellency by placing a 60 μl drop on the surface of a bulk sample and timing its penetration (Doerr *et al.*, 2006).

Wilhelmy plate method
A glass slide of area 3·1 cm^2 was covered with double-sided adhesive tape on all sides followed by a single-grain layer of air-dried minerals. The glass slide was attached to an electronic balance hanging vertically and gradually immersed into water, with the total force F_t (in N) acting on the plate given by Bachmann *et al.* (2003)

$$F_t = W - F_b + F_w = W - V\rho g + l_w \sigma_{lv} \cos\theta \tag{1}$$

where W (kg) denotes the mass of the plate, F_b (N) is the buoyancy force, F_w (N) is the wetting force, V (m^3) is the volume of plate immersed, θ (degrees) is the CA, σ_{lv} (mN/m) is the surface tension of the liquid, g (m/s^2) is acceleration due to gravity, ρ (Mg/m^3) is liquid density and l_w (m) is the wetted length of the sample. If the balance is tared, equation (1) can be rearranged to yield the advancing CA as

$$\cos\theta = \frac{F_t + V\rho g}{l_w \sigma_{lv}} \tag{2}$$

For evaluation of the advancing CA (θ), the wetting force (F_w) has to be determined through linear regression of the recorded weight curve as a function of immersion depth and by extrapolation to zero-depth immersion for F_I (Bachmann *et al.*, 2003). The CAs were measured using a tensiometer (DCAT 11; DataPhysics, Filderstadt, Germany) with an accuracy of ± 5°. One test was conducted for each mineral.

Particle attributes
A dynamic image analyser (QICPIC; Sympatec GmbH, Clausthal-Zellerfeld, Germany) was used to determine the particle attributes. The device comprises a gravity dispenser (GRADIS) and a feeding device (VIBRI) that controls the number of particles in contact with the laser beam per unit time. A series of frames is then captured by means of a camera from which different size and shape descriptors are extracted. The feed and frame rate were adjusted to 15% and 250 Hz, respectively.
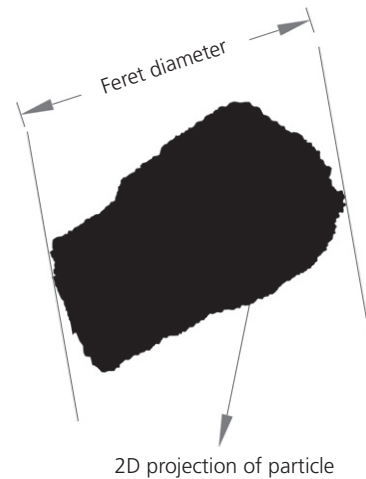

Fig. 1. Definition of Feret diameter from 2D profile

The aspect ratio as defined by QICPIC is the ratio of minimum to maximum Feret diameters, varying between 0 and 1. The Feret diameter is the length between two parallel lines tangential to a particle's silhouette (Fig. 1). The value of sphericity (S) is the ratio of perimeters for a given area (equation (3)) and is equivalent to the 'degree of circularity' defined by Wadell (1933)

$$S = \frac{P_{eqpc}}{P_{real}} \tag{3}$$

in which P_{eqpc} is the perimeter of the equivalent circle and P_{real} is the actual perimeter. From equation (3), it can be deduced that the more the particle's two-dimensional (2D) outline deviates from a circle, the larger P_{real} is. Thus, values of S approaching unity correspond to a shape close to a sphere.

RESULTS AND DISCUSSION
Table 1 shows the CAs for the crushed materials ranked from highest to lowest. The CAs cover a large range, from 164·3° for galena to 0° for quartz. The CAs can be arranged into three groups.

- The sulfides, together with malachite, achieved the highest CA (>99°) with galena consistently achieving the greatest SDM and WPM CAs (>130·6°) and pyrite the lowest (87·3°). This strong water-repellent behaviour was stable over time, as confirmed by the WDPT with the drops in place after 3 h.
- The oxides, together with tourmaline, revealed some water repellency, with CAs ranging between 58·9° (cassiterite) and 99·9° (iron oxide) but dropping to the order of 25° for all oxides after 5 s.
- All silicates, together with calcite, were strongly wettable with initial CAs of the order of 0° (quartz) to 54·7° (calcite).

The CA trends – higher for the sulfides, intermediate for the oxides and lower for the silicates – generally agree with the literature, albeit not in magnitude. For example, for sulfides, Prestidge & Ralston (1995) and Subrahmanyam *et al.* (1996) measured CAs lower than 90° using methods based on capillary pressure equilibrium. Reasons for the discrepancies include oxidation with time of the crushed sulfide surfaces (Prestidge & Ralston, 1996), use of equilibrium CAs for the capillary pressure equilibrium methods, which are always lower than advancing CAs (Prestidge & Ralston, 1995, 1996; Subrahmanyam *et al.*, 1996) and measurements taken on flat

surfaces, which minimises roughness (Raichur *et al.*, 2001). The high CA of malachite is little documented, with Carr (1948) obtaining values in the range 50–90° using different liquids. Maximum CAs for oxides have been reported as 80°, but higher for limonite (~90°) (Maeda *et al.*, 2008) and 74° for hematite and goethite (Iveson *et al.*, 2004). The reported CAs for silicates are generally low, matching this study – 30° for quartz (Fisher & Lark, 1980), 5·6–7·6° for dolomite (a carbonate) (Gence, 2006) and 10° for mica (Bryant *et al.*, 2006). In natural soils, which comprise mineral particles and organic matter, Hajnos *et al.* (2013) reported CAs in the range 2·0–51·8° with the SDM technique.

The CAs were also correlated with particle shape, with more spherical particles achieving higher CAs. The particles' aspect ratios increased from 0·813 to 0·905 and their sphericity from 0·629 to 0·759 for WPM CAs of 0° to 164° (Fig. 2(a)). For the SDM, sphericity increased from 0·813 to 0·875 and aspect ratio from 0·629 to 0·697 for CAs of 17·2°

to 99·9° (Fig. 2(b)). However, high particle attributes did not necessarily equate to high CAs. For instance, the crushed sandstone produced particle attributes of the same range as the sulfides but with lower CAs (>78°) than the sulfides (>120°), while biotite and hematite revealed the opposite. The findings reported by Ulusoy *et al.* (2003) contradict those shown in Figure 2: Ulusoy *et al.* (2003) demonstrated that an increase in roundness (similar to sphericity in the current study) was inversely proportional to the wettability of minerals. A possible reason for this disagreement is the wide range of attributes (0·458 for hematite and 0·759 for galena) whereas the samples in the work of Ulusoy *et al.* deviated from a sphere by at most 10%.

Isolation of material chemistry, layer roughness and particle shape effects on CA measurements is a major challenge. Fundamental studies of surface chemistry and surface thermodynamics have long been applied to thin layers of particles attached to a plane glass surface
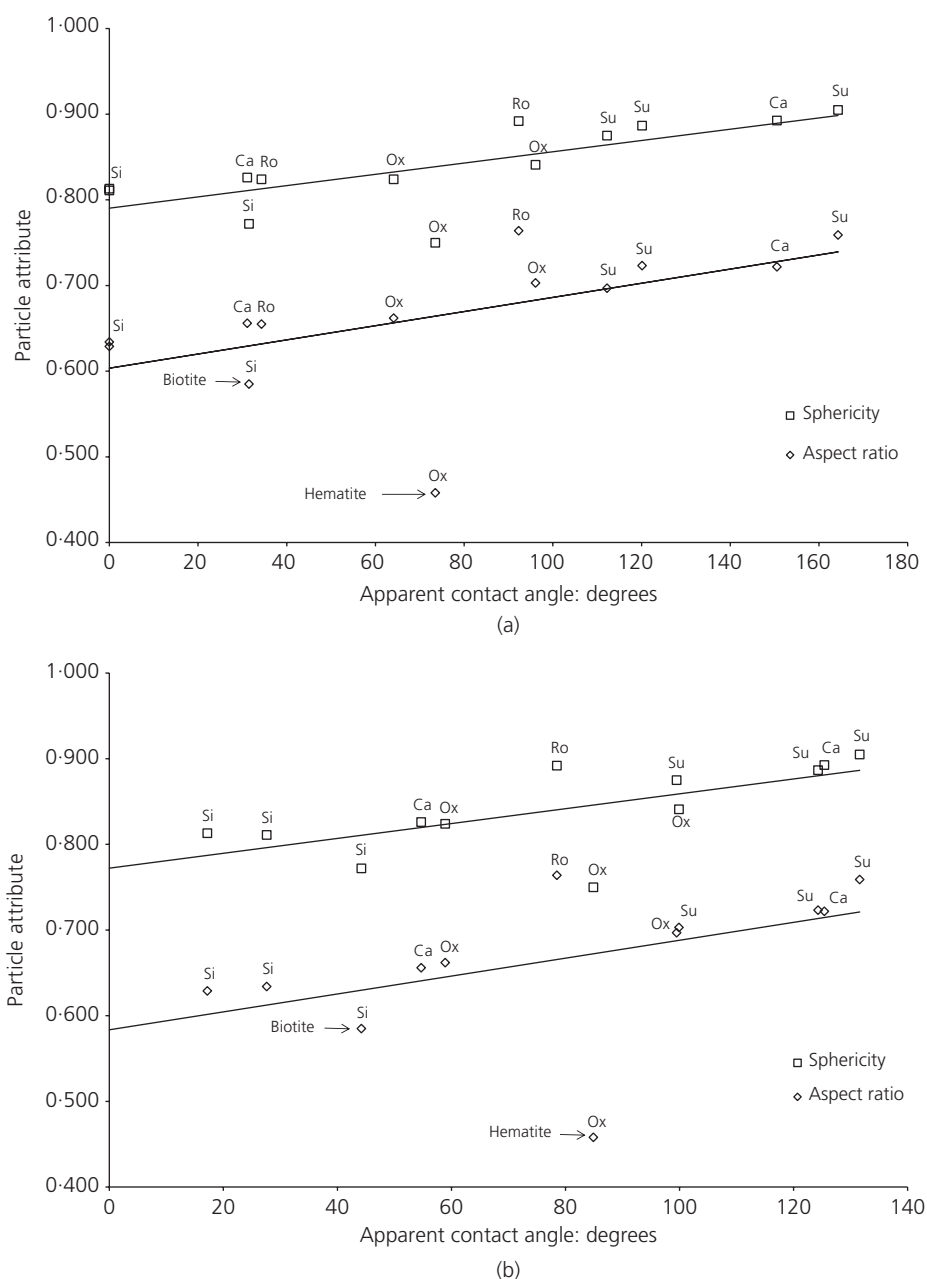

Fig. 2. Particle sphericity and aspect ratio with respect to (a) WPM CAs and (b) SDM CAs. Su, sulfide minerals; Ca, carbonate minerals; Ox, oxide minerals; Si, silicate minerals; Ro, rock samples (including bauxite)

(van Oss *et al.*, 1990). Bachmann *et al.* (2000) proposed fixing soil particles using adhesive tape in order to avoid rearrangement of the particles due to the impact of forces (drop weight, adhesive forces at the three-phase boundary). Model calculations carried out with a combined Wenzel/Cassie–Baxter approach to take into account the simultaneous impact of roughness, particle packing density and chemical heterogeneity showed that the impact of the tape should not be significant (Bachmann & McHale, 2009). In addition, other factors influence the CA, such as particle size (CA increases for finer particles) and, since wettability depends on surfaces characteristics, residual water content and deposition of dust. Given these complexities, one approach to validate CAs is to compare measurements from different methods (as done here). The results revealed broad agreement between the SDM and WPM, with the WPM providing higher and lower CAs at the extremes of wettability.

CONCLUSIONS

The aim of this study was to assess the variability of particle wettability in crushed commonly occurring minerals. The results revealed a wide range of contact angles, with air-dried sulfides and oxides showing water-repellent behaviour. These results suggest that geotechnical processes which generate new surfaces due to particle breakage or abrasion under high stresses (compression or shear) are likely to produce variable surface energies, thus influencing the interaction of the newly formed surfaces with liquids in the post-breakage stage.

ACKNOWLEDGEMENT

REFERENCES

Bachmann, J. & McHale, G. (2009). Superhydrophobic surfaces: a model approach to predict contact angle and surface energy of soil particles. *Euro. J. Soil Sci.* **60**, No. 3, 420–430.

Bachmann, J., Horton, R., van der Ploeg, R. & Woche, S. (2000). Modified sessile drop method for assessing initial soil-water contact angle of sandy soil. *J. Soil Sci. Soc. Am.* **64**, No. 2, 564–567.

Bachmann, J., Woche, S. K., Göbel, M.-O., Kirkham, M. B. & Horton, R. (2003). Extended methodology for determining wetting properties of porous media. *Water Res. Res.* **39**, No. 12, 1353–1366.

Bardet, J. P., Jesmani, M. & Jabbari, N. (2011). Effects of compaction on shear strength of wax-coated sandy soils. *Electron. J. Geotech. Engng* **16**, Bundle D, 451–461.

Bryant, E. M., Bowman, R. S. & Bucley, J. S. (2006). Wetting alteration of mica surfaces with polyethoxylated amine surfactants. *J. Petrol. Sci. Engng* **52**, No. 1–4, 244–252.

Byun, Y.-H., Tran, M. K., Yun, T. S. & Lee, J.-S. (2011). Strength and stiffness characteristics of unsaturated hydrophobic granular media. *ASTM Geotech. Test. J.* **35**, No. 1, 1–8.

Carr, J. S. (1948). *Studies of contact angles on oxidized copper minerals.* Masters thesis. Missouri University of Science and Technology, Rolla, MO, Paper 4943.

Diehl, D., Schneckenburger, T., Krüger, J. *et al.* (2014). Effect of multivalent cations, temperature and aging on soil organic matter interfacial properties. *Environ. Chem.* **11**, No. 6, 709–718.

Doerr, S., Shakesby, R. & Walsh, R. (2000). Soil water repellency: its causes, characteristics and hydro-geomorphological significance. *Earth Sci. Rev.* **51**, No. 1–4, 33–65.

Doerr, S. H., Shakesby, R. A., Dekker, L. W. & Ritsema, C. J. (2006). Occurrence, prediction and hydrological effects of water repellency amongst major soil and land use types in a humid temperate climate. *Eur. J. Soil Sci.* **57**, No. 5, 741–754.

Fisher, L. R. & Lark, P. D. (1980). The effect of adsorbed water vapour on liquid water flow in pyrex glass capillary tubes. *J. Coll. Interf. Sci.* **76**, No. 1, 251–253.

Gence, N. (2006). Wetting behavior of magnesite and dolomite surfaces. *Appl. Surf. Sci.* **252**, No. 10, 3744–3750.

Goebel, M.-O., Woche, S. K., Abraham, P. M., Schaumann, G. E. & Bachmann, J. (2013). Water repellency enhances the deposition of negatively charged hydrophilic colloids in a water-saturated sand matrix. *Coll. Surf. A: Physicochem. Engng Asp.* **431**, 150–160.

Hajnos, M., Calka, A. & Jozefaciuk, G. (2013). Wettability of mineral soils. *Geoderma* **206**, 63–69.

Iveson, S. M., Holt, S. & Biggs, S. (2004). Advancing contact angle of iron ores as a function of their hematite and goethite content: implications for pelletising and sintering. *Int. J. Miner. Proc.* **74**, No. 1–4, 281–287.

Jarvis, N., Etana, A. & Stagnitti, F. (2008). Water repellency, near-saturated infiltration and preferential solute transport in a macroporous clay soil. *Geoderma* **143**, 223–230.

Lourenço, S. D. N., Jones, N., Morley, C., Doerr, S. & Bryant, R. (2015). Hysteresis in the soil water retention of a sand clay mixture with contact angles lower than ninety-degrees. *Vadose Zone J.* **14**, No. 7.

Maeda, T., Fukumoto, C., Matsura, T., Nishioka, K. & Shimizu, M. (2008). Effect of adding moisture and wettability on granulation of iron ore. *ISIJ Int.* **45**, No. 4, 477–484.

Ma'shum, M., Tate, M., Jones, G. & Oades, J. (1988). Extraction and characterization of water-repellent materials. *J. Soil Sci.* **39**, No. 1, 99–110.

Prestidge, C. A. & Ralston, J. (1995). Contact angle studies of galena particles. *J. Coll. Interf. Sci.* **172**, 302–310.

Prestidge, C. A. & Ralston, J. (1996). Contact angle studies of particulate sulphide minerals. *Miner. Engng* **9**, No. 1, 85–102.

Raichur, A. M., Wang, X. H. & Parekh, B. K. (2001). Estimation of surface free energy of pyrites by contact angle measurements. *Miner. Engng* **14**, No. 1, 65–75.

Ritsema, C. & Dekker, L. (1996). Water repellency and its role in forming preferred flow paths in soils. *Aust. J. Soil Res.* **34**, No. 4, 475–487.

Subrahmanyam, T. V., Prestidge, C. A. & Ralston, J. (1996). Contact angle and surface analysis studies of sphalerite particles. *Miner. Engng* **8**, No. 7, 727–741.

Ulusoy, U., Yekeler, M. & Yılmaz, C. (2003). Determination of the shape, morphological and wettability properties of quartz and their correlations. *Miner. Engng* **16**, No. 10, 951–964.

van Oss, C. J., Giese, R. F. & Coslanzo, P. M. (1990). DLVO and non-DLVO interactions in hectorite. *Clays Clay Mineral.* **38**, No. 2, 151–159.

Wadell, H. (1933). Sphericity and roundness of rock particles. *J. Geology* **41**, No. 3, 310–330.

WHAT DO YOU THINK?

To discuss this paper, please email up to 500 words to the editor at journals@ice.org.uk. Your contribution will be forwarded to the author(s) for a reply and, if considered appropriate by the editorial panel, will be published as a discussion.